Hindawi
Advances in Materials Science and Engineering
Volume 2022, Article ID 6111294, 8 pages
https://doi.org/10.1155/2022/6111294

Research Article

The Effects of Temperature and Impact Velocity on the Shock Wave Response of Pore-Embedded Metallic Glasses

Indrajit Patra,[1] **Ahmed M. Abdulhadi**,[2] **Fatima Safaa Fahim**,[3] **Bashar S. Bashar**,[4] **Taif Alawsi**,[5] **and Mohammad Salmani**[6]

[1]*Independent Researcher, Durgapur, West Bengal, India*
[2]*Civil Engineering Department, University of Warith Al-Anbiyaa, Karbala, Iraq*
[3]*Anesthesia Techniques Department, Al-Mustaqbal University College, Babylon, Iraq*
[4]*Al-Nisour University College, Baghdad, Iraq*
[5]*Scientific Research Center, Al-Ayen University, Thi-Qar, Iraq*
[6]*Department of Engineering, Payame Noor University, Tehran Branch, Tehran, Iran*

Correspondence should be addressed to Mohammad Salmani; salmanimohammad253@gmail.com

Received 7 May 2022; Revised 2 June 2022; Accepted 14 June 2022; Published 30 June 2022

Academic Editor: Majid Samavatian

In this work, the shock wave response of a pore-embedded CuZr metallic glass (PEMG) under different impact velocities (0.5–1.5 km/s) and initial temperatures (300–600 K) was evaluated through the molecular dynamics (MD) simulation. The results indicated that the nucleation and growth of nanoscale shear events around the pore were the dominant mechanisms for plastic deformation under the shock wave. It was also found that the increase in the impact velocity led to the filling of pore, which was due to the structural softening and the local temperature increment in the vicinity of pore. Moreover, the spall event originated from the formation and coalescence of tension transformation zones, leading to the formation of nanovoids in the system. At higher velocities, the spallation was accompanied with the formation of more nanovoids with smaller sizes, inducing the brittle failure in the system. The MD outcomes also showed that the increase in initial temperature decreased the shock pressure and flow shear stress and led to the smoother spallation in the PEMG.

1. Introduction

Owing to the absence of long-range orders in their atomic structure, metallic glasses (MGs) exhibit fascinating mechanical properties such as high elastic limit, superior strength, and good self-sharpening [1–4]. Recently, MGs have been also identified as the promising materials for high-velocity impact applications, in which their shock responses grew in considerable importance [5–9]. For instance, Wen et al. [10] reported that the CuZr MGs demonstrates an overdriven plastic state rather than a single elastic shock wave with the piston velocity increasing. It was also found that the increase in Cu content led to the higher resistance to plastic deformation. Li et al. [11] evaluated the shock response of Zr-based MGs under the strain rate of 10^5 s^{-1} and detected some nanocrystals in the impacted specimens. It was also revealed that the rise of impact pressure led to the change of failure mode from spallation to fragmentation accompanied with the combination of spalling cracks and longitudinal cracks. In another study, it was unveiled that the high initial temperature decreased the shear resistance of CuZr BMG under the high-rate loading [12]. Tan et al. [13] carried out the flyer-plate impact experiment and found that the induced stress decreased available free volume under planar impact loading. In this state, the decohesion strength was improved, due to the void coalescence under planar impact loading. Escobedo et al. [14] compared the shock response of two different Zr-based MGs and found that the ZrCuNiAl alloy experienced a higher Hugoniot elastic limit (HEL) and a smooth fracture surface morphology, while the ZrCuAgAl alloy exhibited a rougher fracture surface

with cup-cone features. Wang et al. [15] conducted plate-impact test and figured out that the rise of impact velocity improved the HEL and spall strength. Moreover, they claimed that the MG samples displayed a brittle behavior at macroscopic scale while their microscopic behavior was ductile. In another work, the Hugoniot-compression curve of ZrAlNiCu was measured and the results indicated that a kink was created on the curve at 14 GPa which was due to phase transition in the glassy structure [16].

The effect of embedded pores in the atomic configuration is also one of the main issues in the shock response of MGs. Due to the nanoscale size of pores, the molecular dynamics (MD) simulation has been an efficient method for evaluating the plastic deformation and mechanical properties of porous MGs [17–21]. Using MD simulation, Demaske et al. [22] showed that the mechanism of plastic deformation in the shocked MG is based on the nucleation and growth of shear transformation zones (STZs) around the pores, accompanied with the softening event at the vicinity of pores owing to a regional temperature increment. Song et al. [23] indicated that the void shapes considerably affected the level of atomic strain and fraction of atoms participating in the plastic deformation. They also found that there is no meaningful relation between the void collapse mode and void shape under the weak shocks. In this work, we tried to evaluate the effects of initial temperature and impact velocity on the shock wave response of a pore-embedded MG (PEMG). The results shed light on the design and fabrication of porous MGs for high-strain applications.

2. Computational Method

In general, a wide range of CuZr compositions has been constructed in the MD simulation [24]. In the Cu-rich MGs, the plastic deformation is based on the propagation of main shear bands, while the Zr-rich MGs exhibit a homogenous plasticity with an extensive strain led by the generation of multiple shear events in the structure [25]. Hence, we selected the $Cu_{60}Zr_{40}$ composition which shows a moderate plastic behavior in the CuZr system. In this study, the atomic-scale shock response of $Cu_{60}Zr_{40}$ was characterized through the large-scale atomic/molecular massively parallel simulator package [26]. Moreover, the interaction of Cu and Zr atoms in the structure was described by the embedded-atom method (EAM) potential [27]. At the first step, the $Cu_{60}Zr_{40}$ system with dimensions of $15 \times 15 \times 15$ nm^3 was heated to 2200 K and kept for 1 ns to produce a homogenous melt. Afterward, the system was cooled to the room temperature (300 K) with cooling rate of 10^{11} K/s. The MG cell was then replicated to produce a large specimen with the dimensions of $30 \times 120 \times 120$ nm^3. To ensure the removal of replicating effect, the large sample was again heated to 750 K, relaxed for 300 ps, and cooled back to 300 K. In the end, a spherical pore with a diameter of 20 nm was embedded in a lateral direction into the system (see Figure 1). Again, a similar relaxation treatment was conducted to eliminate the interface effects of embedded pore. It should be noted that the MD simulation was carried out under the three-dimensional periodic boundary conditions, the NPT ensemble, and time step of 2 fs [28, 29].

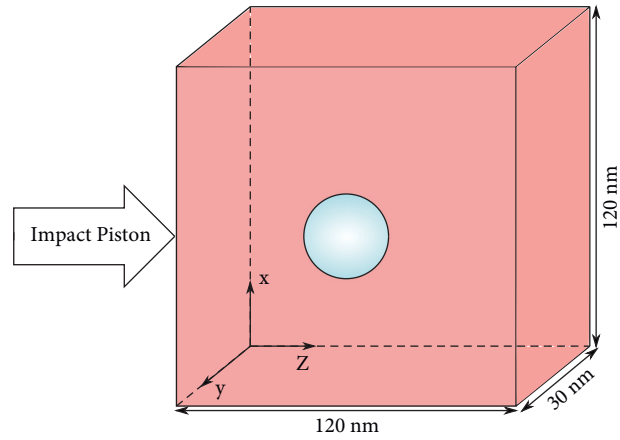

Figure 1: Schematic of PEMG for shock wave process.

After the sample preparation, the shock simulation was performed with the time step of 1 fs in the NVE ensemble under the free boundary conditions in the Z direction and periodic boundary conditions along the X and Y directions. For the shock simulation, an infinite-mass piston with a certain velocity (Up) moved to the MG sample along the Z direction, generating a sudden motion into the system. Consequently, one-dimensional strain with a planar shock wave mode upon a certain velocity (Us) is induced in the MG structure. The impact time was 40 ps and the Up level was set to 0.5–1.5 km/s. Moreover, the initial temperature was in the range of 300–600 K. In the end of impact loading, the piston atoms were unleashed, where the shock wave touched the opposite free surface. At this moment, a rarefaction wave was generated by removal of piston. The total time of shock loading simulation was 100 ps. It is worth mentioning that shock simulation was adopted by the momentum mirror technique [23]. Furthermore, to slice the CuZr MG along the Z direction, 1D binning analysis method was applied through the postprocessing software OVITO [30]. This technique facilitates the thermodynamic and kinetic evaluation of MG structure in each specific bin. To establish a meaningful comparison in the bins, it is also required to subtract the center-of-mass velocity for each bin [31]. The thermodynamic details of microstructure induced by the shock wave are given in [22, 32].

3. Results and Discussion

3.1. Role of Impact Velocity. Firstly, it is required to identify the pore effects on the thermodynamic behavior of PEMGs. Figure 2 represents the distribution of pressure (P_z), shear stress (τ), temperature, and density upon the impact velocity of 1 km/s and initial temperature of 300 K. The results indicated that the elastic wave precursor and the plastic wave front can be distinguished at 20 ps. It is suggested that the Hugoniot elastic limit defines the shock pressure at the point, where the elastic and plastic parts are separated (see

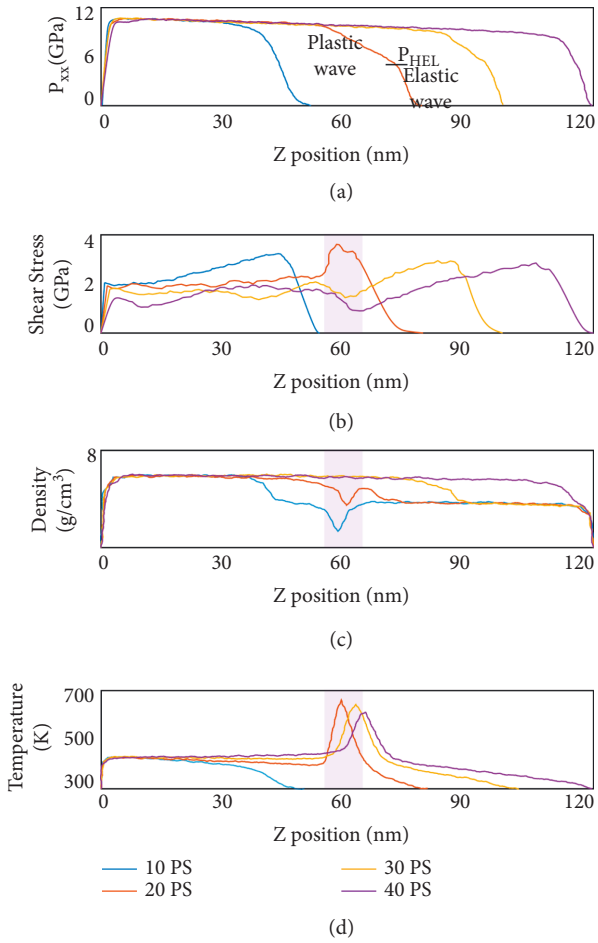

FIGURE 2: The trend of (a) pressure (P_z), (b) shear stress (τ), (c) density, and (d) temperature during the impact time upon the impact velocity of 1 km/s and initial temperature of 300 K.

Figure 2(a)). It should be noted that it is difficult to make a clear distinction between the elastic precursor and plastic front in the MGs [33]. This event becomes highlighted when the pore comes into play and interacts with the shock wave, leading to attenuation of plastic wave propagation in the atomic structure. As can be seen in Figure 2(b), the shear stress exhibited a significant increment in the pore area at 20 ps, which is consistent with the crossing of shock wave from the pore. This outcome means that the atoms are compressed in the pore site and densify this region, as also shown in Figure 2(c). At the time of 20 ps, the temperature of pore site significantly increases to 690 K, which can be due to the sharp movement of atoms at the pore surface (see Figure 2(d)). Previously, it was unveiled that the sharp rearrangement of atoms in the shear bands led to sudden increment of temperature [34]. It seems that the mechanism of temperature alteration in the shear bands is similar to the pore surfaces, where a sudden atomic rearrangement occurs in the system. Passing the time of 20 ps, a shear-stress relaxation occurs in the pore site, implying the intensification of local softening at the vicinity of pores. As also given in Figure 2(c), there is no difference between the density of pore site and its surrounding at 40 ps, demonstrating that the pore is getting filled under the evolution of shock wave through the MG.

The 2D atomic shear strain snapshots of PEMG under different impact velocities are presented in Figure 3. The results indicated that the atomic strain is negligible far from the pore, when the impact velocity is 0.5 km/s. However, some atomic motion in the plastic mode is detected at the vicinity of embedded pore under the evolution shock wave in the bulk of material. It should be noted that the plastic atomic motion mainly occurs perpendicular to the shock wave; however, the pore remains stable without losing its spherical geometry. Hence, it is totally concluded that the atomic response of PEMG can be mainly in an elastic mode at low velocities (0.5 km/s). With the increase of impact velocity to 1 km/s, the pore is nearly filled by the extreme rearrangement of surrounding atoms (40 ps). It is suggested that the filling of pore is accompanied with the generation of shear transformation zones (STZs) in the pore site [23], leading to stress relaxation in this region at 30–40 ps, as also shown in Figure 2(b). Moreover, the results showed that the pore is compressed in the x-axis so that the spherical shape changes to an ellipse configuration. This event proves that a large strain is introduced into the sample perpendicular to the generation of shock wave. At higher impact velocity (1.5 km/s), the glassy structure is exposed to a sharp void collapse owing to the strong shock pressure. In this state, the pore shrinks immediately and an interior jetting event is created along the pressure direction. The interior jetting event induces a hydrodynamic process, leading to sharp atomic compression along the shock direction and significant transfer of kinetic energy from the left side to the right side of the pore [22]. In crystalline materials, the collapse event under the shock wave is based on the dislocation emission from the free surface of pores [35], whereas the mechanism of plastic deformation in porous MGs originated from the formation of STZs around the pore and their generation into the empty space, as shown in Figure 3.

As indicated in Figure 2, the collapse event leads to temperature increment in the material. This primary result suggests that the porous structure may change the temperature behavior of MGs under the shock loading. Figure 4 illustrates the average peak temperature as a function of loading time in the regions with 5 nm thickness around the surface of the pore embedded in the glassy structure. Before the shock wave arrives at the pore site (see stage A in Figure 4), the impact loading itself increases the temperature in the MG structure. When the shock wave reaches the pore site (stage B), the plastic deformation begins in the system and the atoms fill the porous space, leading to significant temperature increment in the structure. At stage C, where the shock wave passes the pore site, the peak temperature declines, which may be due to the relaxation in the system. When the loading time reaches around 60–70 ps, a shoulder in the temperature profile is created (stage D). This shoulder resulted from the arrival of rarefaction waves to the pore site [22]. Finally, the spallation is completed in the system, leading to sharp temperature increment in the structure (stage E). One should note that the rise of impact velocity

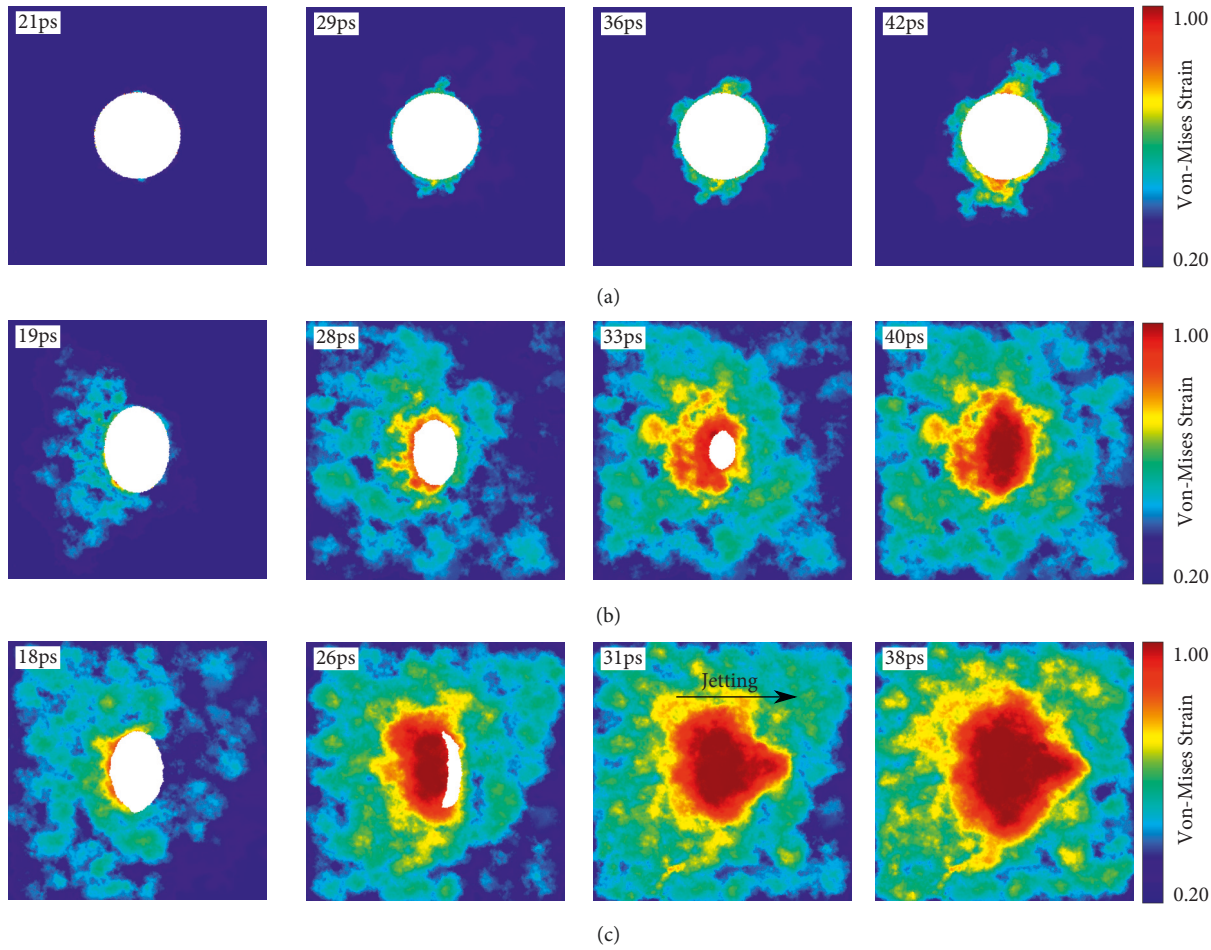

Figure 3: The 2D atomic shear strain snapshots of PEMG under impact velocity of (a) 0.5 km/s, (b) 1 km/s, and (c) 1.5 km/s.

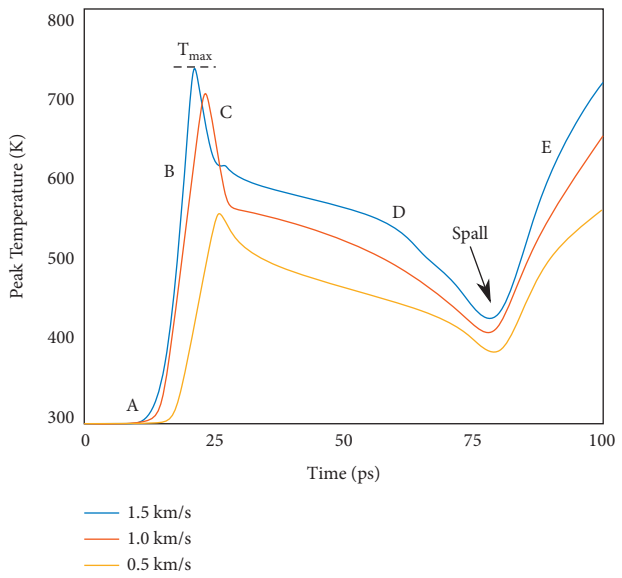

Figure 4: The temperature profile of PEMG under impact velocity of 0.5 km/s, 1 km/s, and 1.5 km/s.

from 1 km/s to 1.5 km/s speeds up the spallation in the system and leads to the intensification of temperature peaks in the pore vicinity. On the other hand, at low velocities (0.5 km/s), the temperature change is negligible, which may be due to the stability of pore geometry under the impact loading.

The plastic deformation of glassy structure under the spallation evolution was studied for the samples exposed to the impact velocities of 1 km/s and 1.5 km/s, in which the pores were filled under the shock wave evolution. Figure 5 indicates the atomic strain snapshots in a thick chunk of sample shocked by a velocity of 1 km/s. At the beginning of spall event, the tension transformation zones (TTZs) nucleate in the structure. It is suggested that the TTZs originated from the rearrangement and annihilation of atomic clusters exposed to the tensile stresses and subsequent sharp dilatation of shear transformation zones (STZs) [36, 37]. Other works also determined that the high-strain state in the shock loading prevents the plastic flow under the generation of STZs and subsequently it induces the fracture of MG through the evolution of TTZs [38]. The TTZs merge into each other and form voids in the system. Finally, the enlargement and coalescence of these voids lead to spall event in the material. Figure 6 illustrates the spallation in the MG structure under impact velocity of 1.5 km/s. As observed, with the increase in impact velocities ($U_p = 1.5$ km/s), the number of TTZs rises and consequently the void growth is restricted to the small sizes. The

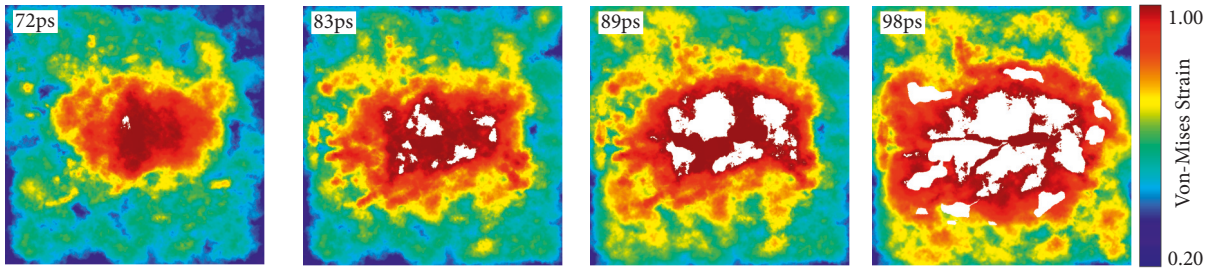

Figure 5: The spall evolution in the sample shocked by the impact velocity of 1 km/s and initial temperature of 300 K.

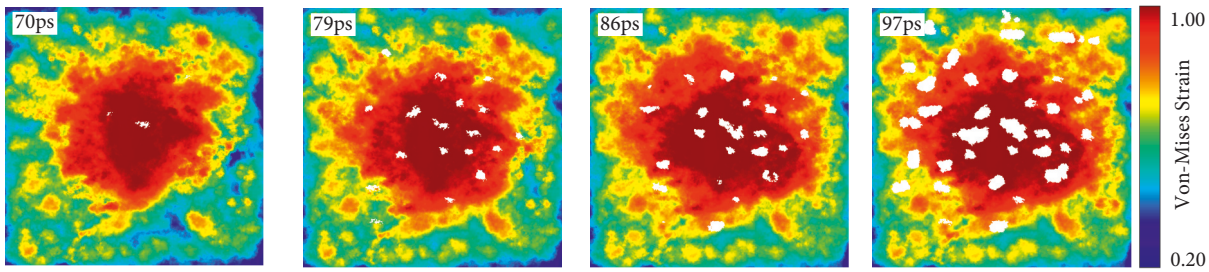

Figure 6: The spall evolution in the sample shocked by the impact velocity of 1.5 km/s and initial temperature of 300 K.

voids also become smaller and are uniformly distributed in the glassy structure at the impact velocity of 1.5 km/s. This outcome determines that there is competition between the void growth and TTZ nucleation with the increase of impact velocity. At lower U_p values, the temperature and strain rate of loading are relatively low, facilitating the stress relaxation and prohibiting the formation of TTZs in the system. On the other hand, the increase of U_p shortens the time of structural relaxation, leading to nucleation of multiple TTZs in the material. The experimental works indicated that creation of numerous small voids under the high impact velocity leads to smoothening of fractured surface in the MGs [39].

3.2. Role of Shock Temperature. Figure 7(a) represents the shear stress and P_z values as a function loading time for the sample shocked by the impact velocity of 1 km/s at room temperature (300 K). The results indicate that the shear stress shows a rapid peak at initial stage of loading and then it drops to a constant value, which is indicative of shear stress flow in the system. Moreover, the critical value of shear stress (τ_{HEL}) is the separator of elastic and plastic regimes under the shock loading. On the other hand, the P_z curve exhibits a two-step trend, in which the first step is associated to the elastic wave and the second step is correlated to the plastic deformation under the shock loading. In general, the pressure in the plastic deformation stage is identified as P_{shock} in the shock loading. Figure 7(b) shows τ_{flow} and P_{shock} as a function of initial temperature. It should be noted that τ_{flow} and P_{shock} values were obtained from the samples shocked through the impact velocities of 0.5–1.5 km/s. The results indicated that the increase in the initial temperature leads to the decline of τ_{flow} and P_{shock} values, meaning that the temperature alteration plays a significant role in the stress distribution. However, one can see that the rate of P_{shock} decrement is sharper than τ_{flow}. This outcome suggests that the shear stress is more dominant at higher temperatures, leading to nucleation and propagation of STZs in the structure, while the TTZ formation is restricted to a few number of sites. Hence, one can conclude that the higher initial temperature facilitates the STZ formation and plastic flow in the system, which causes a smooth spallation with a ductile failure. Figure 8 illustrates the trend of Cu-centered clusters in the samples exposed to the different initial temperatures under the impact velocity of 1 km/s. In general, the Cu-centered clusters are identified as the backbone structure of CuZr MGs and include main polyhedrons in the atomic system [40]. As observed in the figure, the increase in the initial temperature led to the sharp decrement of Cu-centered clusters in the MG structure. This means that higher temperature facilitates the plastic flow and generates the loosely packed regions, i.e., nanoscale free volumes, in the system. Hence, it is found that the plastic deformation is intensified at higher temperatures; however, it originated from the nucleation and propagation of STZ in the structure, as concluded from Figure 7.

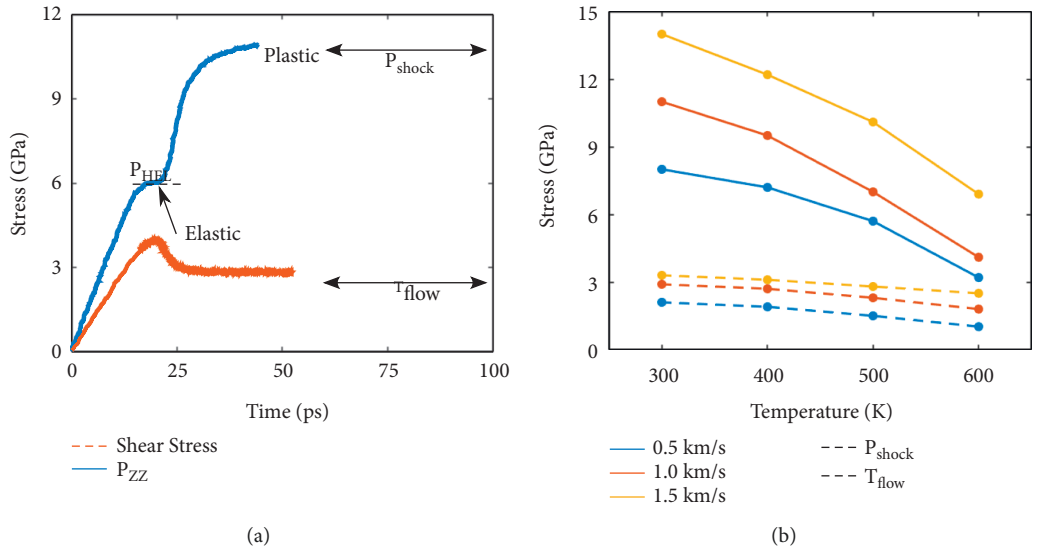

Figure 7: (a) Time dependence of P_z and shear stress τ for impact velocity of 1 km/s and initial temperature of 300 K. (b) Shock pressure and shear-stress flow as a function of initial temperature.

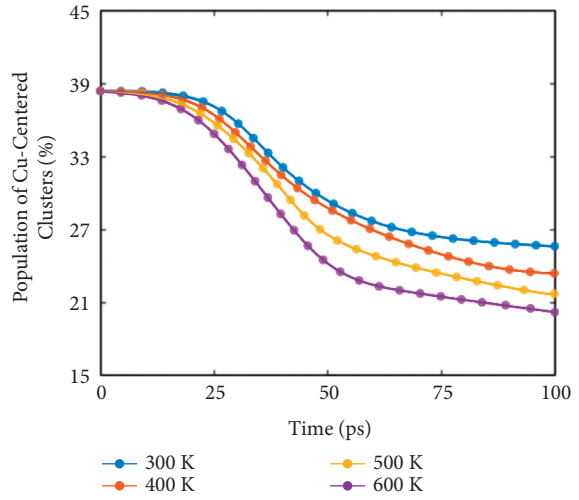

Figure 8: Population of Cu-centered clusters as a function of shock loading time under the impact velocity of 1 km/s and different initial temperatures.

4. Conclusions

In this paper, MD simulation was conducted to study the shock wave response of CuZr PEMG under different initial temperatures and impact velocities. Based on the MD results, the embedded pore was filled under the impact velocities of 1 and 1.5 km/s through the growth of shear events and local softening at the pore boundary. The results also demonstrated that the nucleation and coalescence of TTZs led to the formation of nanovoids under the spall event. The higher velocities induced smaller nanovoids with more population in the strained zones. The initial temperature also played a crucial role in the spall event so that the rise of temperature declined the induced pressure and shear stress in the system, which led to the restriction of TTZ formation and the smoother spallation.

Data Availability

The data used to support the findings of this study are included within the article.

Conflicts of Interest

The authors declare that they have no conflicts of interest.

References

[1] J.-c. Li, X.-w. Chen, and F.-l. Huang, "Ballistic performance of tungsten particle/metallic glass matrix composite long rod," *Defence Technology*, vol. 15, no. 2, pp. 132–145, 2019.

[2] K. Chen, M. Yuan, H. M. Zheng, and S. H. Chen, "On the determination and optimization of apparent "elastic limit" of kirigami metallic glasses," *Physica B: Condensed Matter*, vol. 609, Article ID 412901, 2021.

[3] M. Samavatian, R. Gholamipour, A. A. Amadeh, and S. Mirdamadi, "Correlation between plasticity and atomic structure evolution of a rejuvenated bulk metallic glass," *Metallurgical and Materials Transactions A*, vol. 50, no. 10, pp. 4743–4749, 2019.

[4] W. Bao, J. Chen, X. Yang, T. Xiang, Z. Cai, and G. Xie, "Improved strength and conductivity of metallic-glass-reinforced nanocrystalline CuCrZr alloy," *Materials & Design*, vol. 214, Article ID 110420, 2022.

[5] C. T. Wang, Y. He, C. Ji, Y. He, W. Han, and X. Pan, "Investigation on shock-induced reaction characteristics of a Zr-based metallic glass," *Intermetallics*, vol. 93, pp. 383–388, 2018.

[6] K. V. Reddy, C. Deng, and S. Pal, "Dynamic characterization of shock response in crystalline-metallic glass nanolaminates," *Acta Materialia*, vol. 164, pp. 347–361, 2019.

[7] S. Mishra, K. V. Reddy, and S. Pal, "Impact of crystalline-amorphous interface on shock response of metallic glass Al90Sm10/crystalline Al nanolaminates," *Applied Physics A*, vol. 127, no. 10, p. 774, 2021.

[8] X. C. Tang, C. Li, H. Y. Li et al., "Cup-cone structure in spallation of bulk metallic glasses," *Acta Materialia*, vol. 178, pp. 219–227, 2019.

[9] L. Lu, C. Li, W. H. Wang, M. H. Zhu, X. L. Gong, and S. N. Luo, "Ductile fracture of bulk metallic glass Zr 50 Cu 40 Al 10 under high strain-rate loading," *Materials Science and Engineering*, vol. 651, pp. 848–853, 2016.

[10] P. Wen, B. Demaske, D. E. Spearot, and S. R. Phillpot, "Shock compression of Cu x Zr100−x metallic glasses from molecular dynamics simulations," *Journal of Materials Science*, vol. 53, no. 8, pp. 5719–5732, 2018.

[11] Y. Li, X. Cheng, Z. Ma, X. Li, and M. Wang, "Dynamic response and damage evolution of Zr-based bulk metallic glass under shock loading," *Journal of Materials Science & Technology*, vol. 93, pp. 119–127, 2021.

[12] P. Wen, B. Demaske, D. E. Spearot, S. R. Phillpot, and G. Tao, "Effect of the initial temperature on the shock response of Cu50Zr50 bulk metallic glass by molecular dynamics simulation," *Journal of Applied Physics*, vol. 129, Article ID 165103, 2021.

[13] Y. Tan, Y. W. Wang, H. W. Cheng, and X. W. Cheng, "Dynamic fracture behavior of Zr63Cu12Ni12Al10Nb3 metallic glass under high strain-rate loading," *Journal of Alloys and Compounds*, vol. 853, Article ID 157110, 2021.

[14] J. P. Escobedo, D. J. Chapman, K. J. Laws et al., "Effects of chemical composition on the shock response of Zr-based metallic glasses," *AIP Conference Proceedings*, vol. 1793, Article ID 100032, 2017.

[15] B. P. Wang, L. Wang, S. Wang et al., "Mechanical response of Ti-based bulk metallic glass under plate-impact compression," *Intermetallics*, vol. 63, pp. 12–18, 2015.

[16] T. Mashimo, H. Togo, Y. Zhang et al., "Hugoniot-compression curve of Zr-based bulk metallic glass," *Applied Physics Letters*, vol. 89, no. 24, Article ID 241904, 2006.

[17] X. Q. Lu, L. Li, Y. H. Zhang et al., "Control of shear band formation in metallic glasses through introducing nanoscale pores," *Journal of Non-crystalline Solids*, vol. 569, Article ID 120994, 2021.

[18] N. V. Priezjev and M. A. Makeev, "Strain-induced deformation of the porous structure in binary glasses under tensile loading," *Computational Materials Science*, vol. 150, pp. 134–143, 2018.

[19] H. Liu, Z. Chen, J. Mo, M. Wang, Y. Zhang, and W. Yang, "Brittle-to-ductile transition in monatomic Tantalum nanoporous metallic glass," *Journal of Non-crystalline Solids*, vol. 506, pp. 6–13, 2019.

[20] Y. Luo, G. Yang, Y. Shao, and K. Yao, "The effect of void defects on the shear band nucleation of metallic glasses," *Intermetallics*, vol. 94, pp. 114–118, 2018.

[21] D.-Q. Doan, T.-H. Fang, T.-H. Chen, and T.-X. Bui, "Effects of void and inclusion sizes on mechanical response and failure mechanism of AlCrCuFeNi2 high-entropy alloy," *Engineering Fracture Mechanics*, vol. 252, Article ID 107848, 2021.

[22] B. Demaske, S. R. Phillpot, D. E. Spearot, and P. Wen, "Void collapse and subsequent spallation in Cu50Zr50 metallic glass under shock loading by molecular dynamics simulations," *Journal of Applied Physics*, vol. 125, no. 21, Article ID 215903, 2019.

[23] W. Song, Y. Yu, and Y. Guan, "Role of void shape on shock responses of nanoporous metallic glasses via molecular dynamics simulation," *International Journal of Mechanical Sciences*, vol. 218, Article ID 107076, 2022.

[24] M. Imran, F. Hussain, M. Rashid, Y. Cai, and S. A. Ahmad, "Mechanical behavior of Cu—Zr bulk metallic glasses (BMGs): a molecular dynamics approach," *Chinese Physics B*, vol. 22, Article ID 96101, 2013.

[25] X. X. Yue, C. T. Liu, S. Y. Pan, A. Inoue, P. K. Liaw, and C. Fan, "Effect of cooling rate on structures and mechanical behavior of Cu50Zr50 metallic glass: a molecular-dynamics study," *Physica B: Condensed Matter*, vol. 547, pp. 48–54, 2018.

[26] S. Plimpton, "Fast parallel algorithms for short-range molecular dynamics," *Journal of Computational Physics*, vol. 117, no. 1, pp. 1–19, 1995.

[27] M. I. Mendelev, D. J. Sordelet, and M. J. Kramer, "Using atomistic computer simulations to analyze x-ray diffraction data from metallic glasses," *Journal of Applied Physics*, vol. 102, Article ID 43501, 2007.

[28] P. Gupta, S. Pal, and N. Yedla, "Molecular dynamics based cohesive zone modeling of Al (metal)-Cu50Zr50 (metallic glass) interfacial mechanical behavior and investigation of dissipative mechanisms," *Materials & Design*, vol. 105, pp. 41–50, 2016.

[29] T. Bučko and F. Šimko, "On the structure of crystalline and molten cryolite: insights from the ab initio molecular dynamics in NpT ensemble," *The Journal of Chemical Physics*, vol. 144, Article ID 064502, 2016.

[30] A. Stukowski, "Visualization and analysis of atomistic simulation data with OVITO–the Open Visualization Tool," *Modelling and Simulation in Materials Science and Engineering*, vol. 18, Article ID 0, 2009.

[31] J.-L. Shao, C. Wang, P. Wang, A.-M. He, and F.-G. Zhang, "Atomistic simulations and modeling analysis on the spall damage in lead induced by decaying shock," *Mechanics of Materials*, vol. 131, pp. 78–83, 2019.

[32] F. Shimizu, S. Ogata, and J. Li, "Theory of shear banding in metallic glasses and molecular dynamics calculations," *Materials Transactions*, vol. 48, no. 11, pp. 2923–2927, 2007.

[33] B. J. Demaske, P. Wen, S. R. Phillpot, and D. E. Spearot, "Atomic-level deformation of Cu x Zr100-x metallic glasses under shock loading," *Journal of Applied Physics*, vol. 123, Article ID 215101, 2018.

[34] J. J. Lewandowski and A. L. Greer, "Temperature rise at shear bands in metallic glasses," *Nature Materials*, vol. 5, no. 1, pp. 15–18, 2006.

[35] L. P. Davila, P. Erhart, E. M. Bringa et al., "Atomistic modeling of shock-induced void collapse in copper," *Applied Physics Letters*, vol. 86, Article ID 161902, 2005.

[36] M. Q. Jiang, Z. Ling, J. X. Meng, and L. H. Dai, "Energy dissipation in fracture of bulk metallic glasses via inherent competition between local softening and quasi-cleavage," *Philosophical Magazine*, vol. 88, no. 3, pp. 407–426, 2008.

[37] C. Minnert, M. Kuhnt, S. Bruns et al., "Study on the embrittlement of flash annealed Fe85.2B9.5P4Cu0.8Si0.5 metallic glass ribbons," *Materials & Design*, vol. 156, pp. 252–261, 2018.

[38] X. Zhang, W. Li, Y. Deng, J. Shao, X. Zhang, and L. Chen, "Strength criterion and temperature dependent strength model of metallic glasses," *International Journal of Solids and Structures*, vol. 163, pp. 242–251, 2019.

[39] H. Jia, G. Wang, S. Chen, Y. Gao, W. Li, and P. K. Liaw, "Fatigue and fracture behavior of bulk metallic glasses and their composites," *Progress in Materials Science*, vol. 98, pp. 168–248, 2018.

[40] Y.-L. Guan, L.-S. Dai, J.-L. Shao, and W.-D. Song, "Molecular dynamics study on the nanovoid collapse and local deformation in shocked Cu50Zr50 metallic glasses," *Journal of Non-Crystalline Solids*, vol. 559, Article ID 120703, 2021.